

Fig. 10.16. A specimen of alumina (a) sintered 1 hr at 1800°C and (b) heated 1 hr at 1900°C to give secondary recrystallization. Note that the pore spacing has not changed. Courtesy J. E. Burke.

preferred orientation increased to 93% alignment, corresponding to the structural change brought about by secondary recrystallization. It seems apparent that the few large grains in the starting material are more uniformly aligned than the fine surrounding material. These grains serve as nuclei for the secondary recrystallization process and give rise to a highly oriented final product.

## 10.2 Solid-State Sintering

Changes that occur during the firing process are related to (1) changes in grain size and shape, (2) changes in pore shape, and (3) changes in pore size. In Section 10.1 we concentrated on changes in grain size; in this and the following section we are mainly concerned with changes in porosity, that is, the changes taking place during the transformation of an originally porous compact to a strong, dense ceramic. As formed, a powder compact, before it has been fired, is composed of individual grains separated by between 25 and 60 vol% porosity, depending on the particular material used and the processing method. For maximizing properties such as strength, translucency, and thermal conductivity, it is desirable to eliminate as much of this porosity as possible. For some other applications it may be desirable to increase this strength without decreasing the gas permeability. These results are obtained during firing by the transfer of material from one part of the structure to the other. The kind of changes that may occur are illustrated in Fig. 10.17. The pores initially present can change shape, becoming channels or isolated spheres, without necessarily changing in size. More commonly, however, both the size and shape of the pores present change during the firing process, the pores becoming more spherical in shape and smaller in size as firing continues.

**Driving Force for Densification.** The free-energy change that gives rise to densification is the decrease in surface area and lowering of the surface free energy by the elimination of solid-vapor interfaces. This usually takes place with the coincidental formation of new but lower-energy

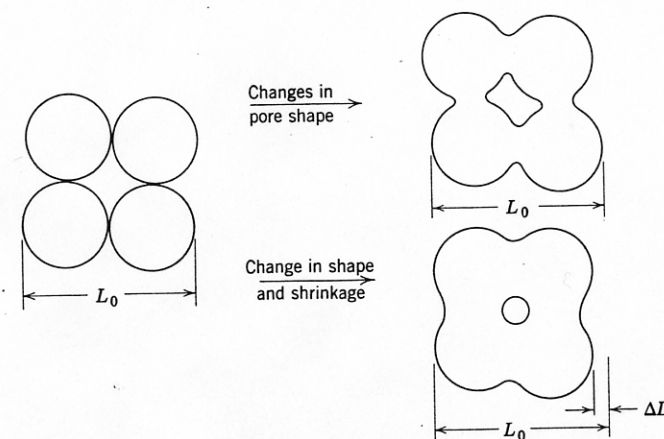


Fig. 10.17. Changes in pore shape do not necessarily require shrinkage.

solid-solid interfaces. The net decrease in free energy occurring on sintering a 1-micron particle size material corresponds to an energy decrease of about 1 cal/g. On a microscopic scale, material transfer is affected by the pressure difference and changes in free energy across a curved surface. These changes are due to the surface energy and have been discussed in Chapter 5 and referred to in Section 10.1. If the particle size, and consequently the radius of curvature, is small, these effects may be of a substantial magnitude. As indicated in Chapter 5, they become large when the radius of curvature is less than a few microns. This is one of the major reasons why much ceramic technology is based on and depends on the use of fine-particle materials.

Most of the insight into the effect of different variables on the sintering process has come from considering simple systems and comparing experimental data with simple models. Since our major aim is to be sure we understand the importance of different variables in traditional or new systems, we use this method here. Since the driving force is the same (surface energy) in all systems, considerable differences in behavior in various types of systems must be related to different mechanisms of material transfer. Several can be imagined—evaporation and condensation, viscous flow, surface diffusion, grain-boundary or lattice diffusion, and plastic deformation are among those that occur to us. Of these, diffusion and viscous flow are important in the largest number of systems; evaporation-condensation is perhaps the easiest to visualize.

**Evaporation-Condensation.** During the sintering process there is a tendency for material transfer because of the differences in surface curvature and consequently the differences in vapor pressure at various parts of the system. Material transfer brought about in this way is only important in a few systems; however, it is the simplest sintering process to treat quantitatively. We derive the sintering rate in some detail, since it provides a sound basis for understanding more complex processes.

Let us consider the initial stages of the process when the powder compact is just beginning to sinter and concentrate on the interaction between two adjacent particles (Fig. 10.18). At the surface of the particle there is a positive radius of curvature so that the vapor pressure is somewhat larger than would be observed for a flat surface. However, just at the junction between particles there is a neck with a small negative radius of curvature and a vapor pressure an order of magnitude lower than that for the particle itself. The vapor-pressure difference between the neck area and the particle surface tends to transfer material into the neck area.

We can calculate the rate at which the bonding area between particles increases by equating the rate of material transfer to the surface of the

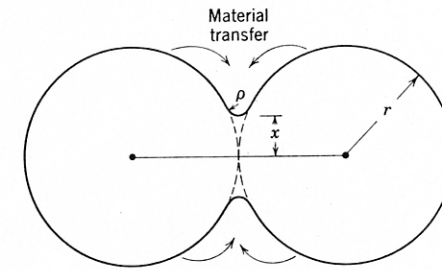


Fig. 10.18. Initial stages of sintering by evaporation-condensation.

lens between the spheres with the increase in its volume. The vapor pressure over the small negative radius of curvature is decreased because of the surface energy in accordance with the Thomson-Freundlich (Kelvin) equation discussed in Chapter 5:

$$\ln \frac{p_1}{p_0} = \frac{\gamma M}{dRT} \left( \frac{1}{\rho} + \frac{1}{x} \right) \quad (10.14)$$

where  $p_1$  is the vapor pressure over the small radius of curvature,  $M$  is the molecular weight of the vapor, and  $d$  is the density. In this case the neck radius is much larger than the radius of curvature at the surface,  $\rho$ , and the pressure difference  $p_0 - p_1$  is small. Consequently, to a good approximation,  $\ln p_1/p_0$  equals  $\Delta p/p_0$ , and we can write

$$\Delta p = \frac{\gamma M p_0}{d \rho RT} \quad (10.15)$$

where  $\Delta p$  is the difference between the vapor pressure of the small negative radius of curvature and the saturated vapor in equilibrium with the nearly flat particle surfaces. The rate of condensation is proportional to the difference in equilibrium and atmospheric vapor pressure and is given by the Langmuir equation to a good approximation as

$$m = \alpha \Delta p \left( \frac{M}{2\pi RT} \right)^{1/2} \quad \text{g/cm}^2/\text{sec} \quad (10.16)$$

where  $\alpha$  is an accommodation coefficient which is nearly unity. Then the rate of condensation should be equal to the volume increase. That is,

$$\frac{mA}{d} = \frac{dv}{dt} \quad \text{cm}^3/\text{sec} \quad (10.17)$$

From the geometry of the two spheres in contact, the radius of curvature at the contact points is approximately equal to  $x^2/2r$  for  $x/r$  less than 0.3;



the area of the surface of the lens between spheres is approximately equal to  $\pi^2 x^3/r$ ; the volume contained in the lenticular area is approximately  $\pi x^4/2r$ . That is,

$$\rho = \frac{x^2}{2r}; \quad A = \frac{\pi^2 x^3}{r}; \quad v = \frac{\pi x^4}{2r} \quad (10.18)$$

Substituting values for  $m$  in Eq. 10.16,  $A$  and  $v$  in Eq. 10.18 into Eq. 10.17 and integrating, we obtain a relationship for the rate of growth of the bond area between particles:

$$\frac{x}{r} = \left( \frac{3\sqrt{\pi}\gamma M^{3/2} p_0}{\sqrt{2} R^{3/2} T^{3/2} d^2} \right)^{1/3} r^{-2/3} t^{1/3} \quad (10.19)$$

This equation gives the relationship between the diameter of the contact area between particles and the variables influencing its rate of growth.

The important factor from the point of view of strength and other material properties is the bond area in relation to the individual particle size, which gives the fraction of the projected particle area which is bonded together—the main factor in fixing strength, conductivity, and related properties. As seen from Eq. 10.19, the rate at which the area between particles forms varies as the two-thirds power of time. Plotted on a linear scale, this decreasing rate curve has led to characterizations of *end point* conditions corresponding to a certain sintering time. This concept of an end point is useful, since periods of time for sintering are not widely changed; however, the same rate law is observed for the entire process (Fig. 10.19b).

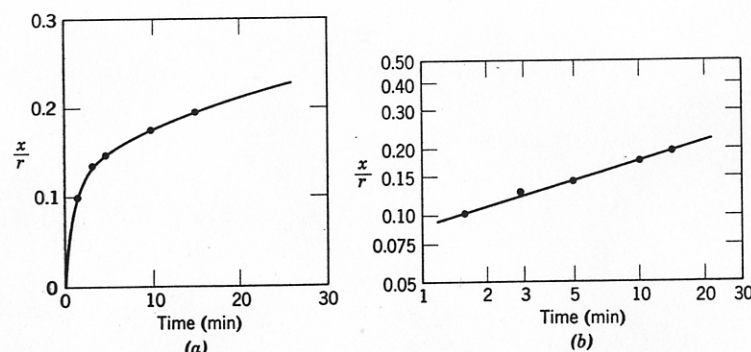


Fig. 10.19. (a) Linear and (b) log-log plots of neck growth between spherical particles of sodium chloride at 725°C.

If we consider the changes in structure that take place during a process such as this, it is clear that the distance between centers of spherical particles (Fig. 10.18) is not affected by the transfer of material from the particle surface to the interparticle neck. This means that the total shrinkage of a row of particles, or of a compact of particles, is unaffected by vapor-phase-material transfer and that only the shape of pores is changed. This changing shape of pores can have an appreciable effect on properties but does not affect density.

The principal variables in addition to time that affect the rate of pore-shape change through this process are the initial particle radius (rate proportional to  $1/r^{2/3}$ ) and the vapor pressure (rate proportional to  $p_0^{1/3}$ ). Since the vapor pressure increases exponentially with temperature, the process of vapor-phase sintering is strongly temperature-dependent. From a processing point of view, the two main variables over which control can be exercised for any given material are the initial particle size and the temperature (which fixes the vapor pressure). Other variables are generally not easy to control, nor are they strongly dependent on conditions of use.

The negligible shrinkage corresponding to vapor-phase-material transfer is perhaps best illustrated in Fig. 10.20, which shows the shape changes that occur on heating a row of initially spherical sodium chloride particles. After long heating the interface contact area has increased; the

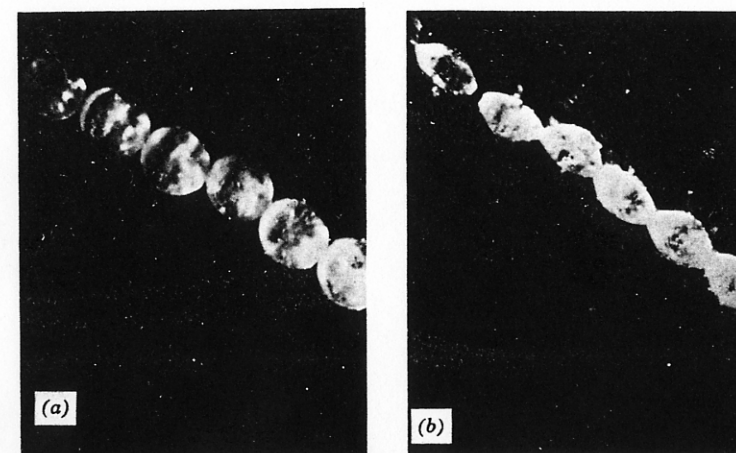


Fig. 10.20. Photomicrographs of sintering sodium chloride at 750°C: (a) 1 min; (b) 90 min.

particle diameter has been substantially decreased, but the distance between particle centers, that is, the shrinkage, has not been affected.

Vapor-phase material transfer requires that materials be heated to a temperature sufficiently high for the vapor pressure to be appreciable. For micron-range particle sizes this requires vapor pressures in the order of  $10^{-4}$  to  $10^{-5}$  atm, a pressure higher than those usually encountered during sintering of oxide and similar phases. Vapor-phase transfer plays an important part in the changes occurring during treatment of halides such as sodium chloride and is important for the changes in configuration observed in snow and ice technology.

**Solid-State Processes.** The difference in free energy or chemical potential between the neck area and the surface of the particle provides a driving force which causes the transfer of material by the fastest means available. If the vapor pressure is low, material transfer may occur more readily by solid-state processes, several of which can be imagined. As shown in Fig. 10.21 and Table 10.1, in addition to vapor transport (process 3), matter can move from the particle surface, from the particle bulk, or from the grain boundary between particles by surface, lattice, or grain-boundary diffusion. Which one or more of these processes actually contributes significantly to the sintering process in a particular system depends on their relative rates, since each is a parallel method of lowering the free energy of the system (parallel reaction paths have been discussed in Chapter 9). There is a most significant difference between these paths for matter transport: the transfer of material from the surface to the neck by surface or lattice diffusion, like vapor transport, does not lead to any decrease in the distance between particle centers. That is, these processes do not result in shrinkage of the compact and a decrease in porosity. Only

Table 10.1. Alternate Paths for Matter Transport During the Initial Stages of Sintering<sup>a</sup>

Mechanism Number	Transport Path	Source of Matter	Sink of Matter
1	Surface diffusion	Surface	Neck
2	Lattice diffusion	Surface	Neck
3	Vapor transport	Surface	Neck
4	Boundary diffusion	Grain boundary	Neck
5	Lattice diffusion	Grain boundary	Neck
6	Lattice diffusion	Dislocations	Neck

<sup>a</sup>See Fig. 10.21.

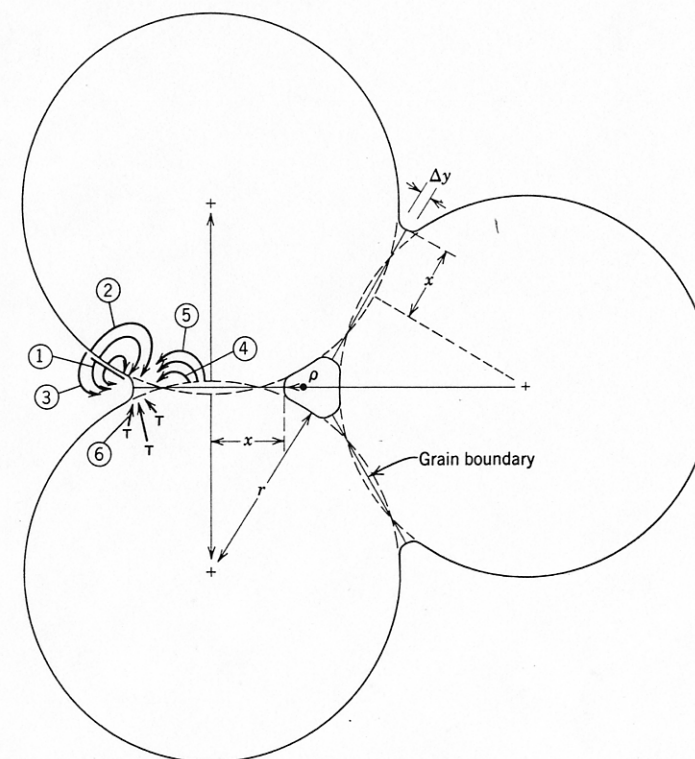


Fig. 10.21. Alternate paths for matter transport during the initial stages of sintering. Courtesy M. A. Ashby. (See Table 10.1.)

transfer of matter from the particle volume or from the grain boundary between particles causes shrinkage and pore elimination.

Let us consider mechanism 5, matter transport from the grain boundary to the neck by lattice diffusion. Calculation of the kinetics of this process is exactly analogous to determination of the rate of sintering by a vapor-phase process. The rate at which material is discharged at the surface area is equated to the increase in volume of material transferred. The geometry is slightly different:

$$\rho = \frac{x^2}{4r}; \quad A = \frac{\pi^2 x^3}{2r}; \quad V = \frac{\pi x^4}{4r} \quad (10.20)$$

The process can be visualized most easily by considering the rate of



migration of vacancies. In the same way that there are differences in vapor pressure between the surface of high negative curvature and the nearly flat surfaces, there is a difference in vacancy concentration. If  $c$  is the concentration of vacancies and  $\Delta c$  is the excess concentration over the concentration on a plane surface  $c_0$ , then, equivalent to Eq. 10.15,

$$\Delta c = \frac{\gamma a^3 c_0}{kT\rho} \quad (10.21)$$

where  $a^3$  is the atomic volume of the diffusing vacancy and  $k$  is the Boltzmann constant. The flux of vacancies diffusing away from the neck area per second per centimeter of circumferential length under this concentration gradient can be determined graphically and is given by

$$J = 4D_v \Delta c \quad (10.22)$$

Where  $D_v$  is the diffusion coefficient for vacancies,  $D_v$  equals  $D^*/a^3 c_0$  if  $D^*$  is the self-diffusion coefficient. Combining Eqs. 10.22 and 10.21 with the continuity equation similar to Eq. 10.17, we obtain the result

$$\frac{x}{r} = \left( \frac{40\gamma a^3 D^*}{kT} \right)^{1/5} r^{-3/5} t^{1/5} \quad (10.23)$$

With diffusion, in addition to the increase in contact area between particles, there is an approach of particles centers. The rate of this approach is given by  $d(x^2/2r)/dt$ . Substituting from Eq. 10.23, we obtain

$$\frac{\Delta V}{V_0} = \frac{3\Delta L}{L_0} = 3 \left( \frac{20\gamma a^3 D^*}{\sqrt{2}kT} \right)^{2/5} r^{-6/5} t^{2/5} \quad (10.24)$$

These results indicate that the growth of bond formation between particles increases as a one-fifth power of time (a result which has been experimentally observed for a number of metal and ceramic systems) and that the shrinkage of a compact densified by this process should be proportional to the two-fifths power of time. The decrease in densification rate with time gives rise to an apparent end-point density if experiments are carried out for similar time periods. However, when plotted on a log-log basis, the change in properties is seen to occur as expected from Eq. 10.24. Experimental data for sodium fluoride and aluminum oxide are shown in Fig. 10.22.

The relationships derived in Eqs. 10.23 and 10.24 and similar relationships for the alternate matter transport processes, which we shall not derive, are important mainly for the insight that they provide on the variables which must be controlled in order to obtain reproducible processing and densification. It is seen that the sintering rate steadily decreases with time, so that merely sintering for longer periods to obtain

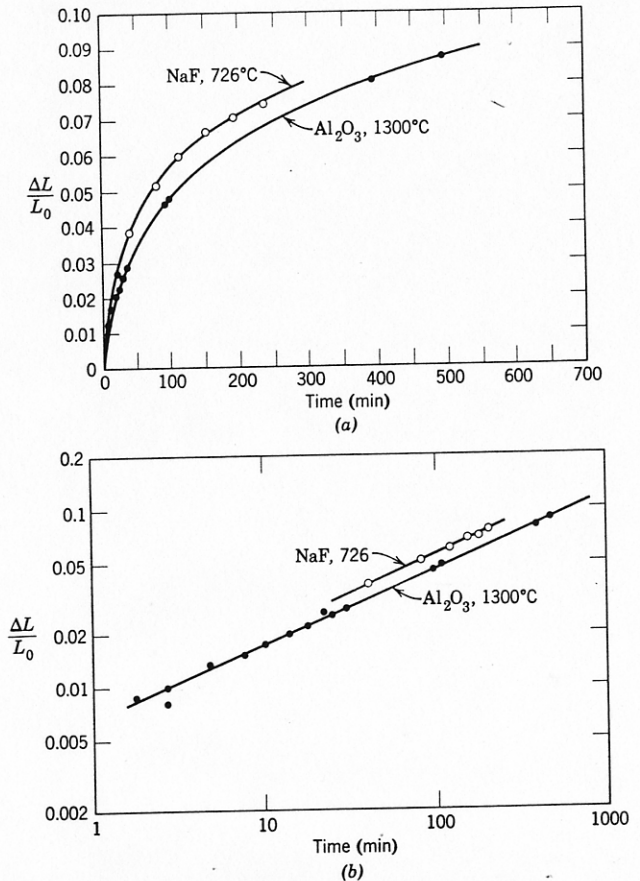


Fig. 10.22. (a) Linear and (b) log-log plots of shrinkage of sodium fluoride and aluminum oxide compacts. From J. E. Burke and R. L. Coble.

improved properties is impracticable. Therefore, time is not a major or critical variable for process control.

Control of particle size is very important, since the sintering rate is roughly proportional to the inverse of the particle size. The interface diameter achieved after sintering for a period of 100 hr at 1600°C is illustrated in Fig. 10.23 as a function of particle size. For large particles even these long periods do not cause extensive sintering; as the particle size is decreased, the rate of sintering is raised.